AIP | Applied Physics Letters

Polarization-dependent light-induced thermionic electron emission from carbon nanotube arrays using a wide range of wavelengths

Mehran Vahdani Moghaddam, Parham Yaghoobi, and Alireza Nojeh

Citation: Appl. Phys. Lett. **101**, 253110 (2012); doi: 10.1063/1.4772504
View online: http://dx.doi.org/10.1063/1.4772504
View Table of Contents: http://apl.aip.org/resource/1/APPLAB/v101/i25
Published by the American Institute of Physics.

Polarization-dependent light-induced thermionic electron emission from carbon nanotube arrays using a wide range of wavelengths

Mehran Vahdani Moghaddam,[a] Parham Yaghoobi,[a] and Alireza Nojeh[b]
Department of Electrical and Computer Engineering, The University of British Columbia, Vancouver, British Columbia V6T 1Z4, Canada

(Received 6 September 2012; accepted 3 December 2012; published online 20 December 2012)

Light-induced thermionic electron emission from arrays of carbon nanotubes is observed using low-power, continuous-wave lasers with a broad set of wavelengths ranging from violet to infrared. The thermionic emission current is highest when the electric field of the laser is parallel to the axis of the nanotubes and lowest when it is perpendicular. The polarization dependence is stronger for the longer-wavelength beam. © *2012 American Institute of Physics*.
[http://dx.doi.org/10.1063/1.4772504]

Light-induced electron emission has a wide variety of applications, ranging from time-resolved electron microscopy[1] to free-electron lasers,[2] and more recently, modern solar energy conversion devices.[3] Photocathodes typically either require high-photon-energy laser sources (ultra-violet) or have to be made from semimetals/semiconductors combined with alkali metals to have low workfunction in order to operate with visible light.[4] The former suffer from the challenges associated with generating high-energy photons and the latter are usually highly unstable and can only operate in ultra high vacuum conditions. High-power pulsed lasers (with a few GW/cm^2 of light intensity) are also used for thermionic electron emission from metals, but again typically require a sophisticated laser source.

Due to the interesting physical properties of carbon nanotubes (CNTs) such as their high aspect ratio and spatially confined nature of charge carriers resulting in strong optical and electrical anisotropy,[5,6] their interaction with laser light has sparked considerable interest. Previously, we reported thermionic emission from carbon nanotube forests (arrays of vertically aligned carbon nanotubes) induced by a beam of continuous-wave green laser.[7,8] In particular, we showed that based on an effect, which we call "Heat Trap," a spot on the surface of the nanotube forest can be effectively thermally isolated from the rest of the surface and efficiently heated to thermionic electron emission temperatures using a laser beam with very low power.[8] Here, we report on the broadband nature and polarization dependence of this light-induced thermionic electron emission effect. We use lasers in a broad visible/infra-red range (405 nm, 514.5 nm, 658 nm, and 1064 nm) and show that the laser driven thermionic emission current is at its maximum when the electric field of the laser is parallel to the axis of the nanotubes (s-polarization). We also show that the polarization dependence is stronger for the longer-wavelength laser; while similar levels of emission current can be obtained using different wavelengths when the beams are s-polarized, at longer wavelengths p-polarized light becomes significantly less effective. These findings could have important implications on light-controlled electron sources for various vacuum electronic applications.

Multi-walled CNT forests were synthesized using ethylene-based chemical vapor deposition. As catalyst, 10 nm of alumina and 1–2 nm of iron were evaporated on a highly doped silicon wafer. The chips were annealed at 800 °C with flows of H_2 and Ar at 800 sccm and 1500 sccm, respectively, which were preheated to 850 °C. Immediately after annealing, 400 sccm of C_2H_4 was introduced and CNT forests of about 2 mm in height were obtained after 20 min of growth.

The chips containing CNT forests were mounted on a sample holder and placed in a high vacuum chamber ($\sim 10^{-8}$ Torr). The forest was used as the cathode and a stainless steel fine mesh anode was placed 1 mm above the forest. A Keithley 6430 source/ammeter was used to apply the collection voltage (10 V) and measure the emission current through the cathode. Three of the lasers used were from Laserglow Technologies with the following model numbers: Electra Pro-40 (405 nm), Orion-200 (658 nm), and Scorpius-500 (1064 nm). The 514.5-nm line was obtained from a vertically polarized Spectra-Physics Beamlok 2060-10 W argon ion laser operated in the single-mode regime using electronics (Z-lock and J-lock). Each beam was passed through a polarizer with an extinction ratio of $>1000:1$ to determine and fix the polarization. A half-wave plate was used to change the angle of polarization between 0° and 90°. An aperture was used to block stray rays that were caused by reflection from the optical components. In all cases, the laser beam was perpendicular to the surface of the sidewall of the forest. The experimental arrangement is illustrated in Figure 1.

Upon irradiation by a laser beam with enough intensity, the illuminated spot on the nanotube forest surface would exhibit a bright incandescent glow, accompanied by electron emission. We have previously shown that the spectrum of the incandescent glow fits the black-body radiation formula for the corresponding temperature.[8]

Figure 2 shows the electron emission current as a function of laser power for four s-polarized (electric field of the laser parallel to the CNT axis) laser beams with different wavelengths. We observe that significant electron emission takes place regardless of the laser wavelength. Since this emission process depends on light intensity, the visible laser beams were characterized for their profile and spot area. All three visible beams had an elliptical shape with the

[a]M. Vahdani Moghaddam and P. Yaghoobi contributed equally to this work.
[b]Electronic mail: anojeh@ece.ubc.ca.

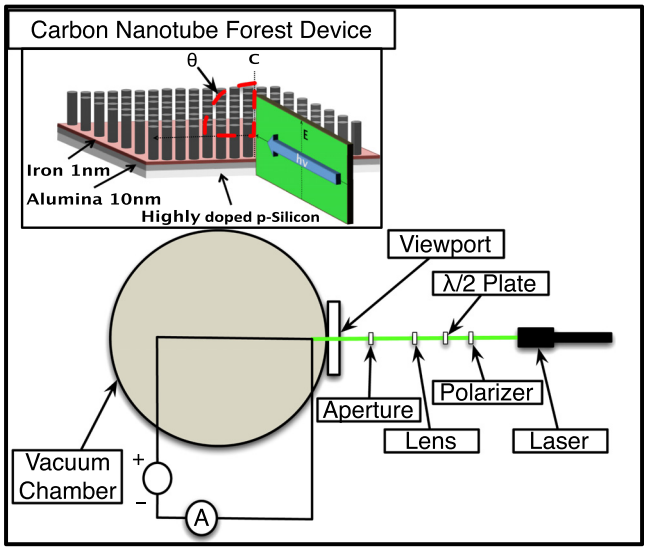

FIG. 1. Schematic of the experimental apparatus using a laser beam focused with a lens (placed outside of the vacuum chamber) on the sidewall of the nanotube forest through a sapphire viewport. Inset shows the polarization angle.

514.5-nm and 658-nm spots having ~0.8× and ~3.4× the area of the 405-nm spot, respectively. By scaling the horizontal axis of the 405-nm curve in Figure 2 by these ratios, we will observe that the emission current resulting from the different laser wavelengths will be approximately the same for the same level of optical power per unit area. Therefore, a broad range of lasers can be used for a nanotube-based thermionic electron-source. It should also be noted that since the emission process is primarily not wavelength dependent, one expects that a regular wide-spectrum light source could also be used. This has important implications for bringing photocathodes to mainstream applications such as solar energy conversion and displays.

The Richardson plot, the logarithm of $\frac{I}{T^2}$ as a function of $\frac{1}{T}$, is shown for all laser wavelengths in order to confirm whether the electron emission here follows the thermionic emission law, and a reasonable match is found over a wide temperature range of 1650–2200 K (Figure 3).

The effect of combined wavelengths can be demonstrated by focusing the different beams onto a single spot (Figure 4(a)). As illustrated in Table I, the emission current due to the combination of the laser beams is much higher than the sum of currents resulting from each laser independently. For example, the emission current due to the combination of green and red is about 2 orders of magnitude higher than the currents due to red and green added together. Such non-linearity is, of course, expected in thermionic emission, where the addition of a small amount of laser power and corresponding rise in temperature could lead to a significant increase in current. To further illustrate this point, Figure 4(b) shows the emission current as a function of calculated temperature using the power equilibrium condition discussed in our previous work[8] and Richardson's equation.[9] In order to estimate the temperature for the combination of green + red and green + red + violet, only the total power of the different lasers was used (regardless of their wavelength). For example, to estimate the temperature of the green + red combination, a power of 45 mW + 150 mW was used. As it can be seen in Figure 4(b), the trend of increase in current for the different combinations of lasers follows the

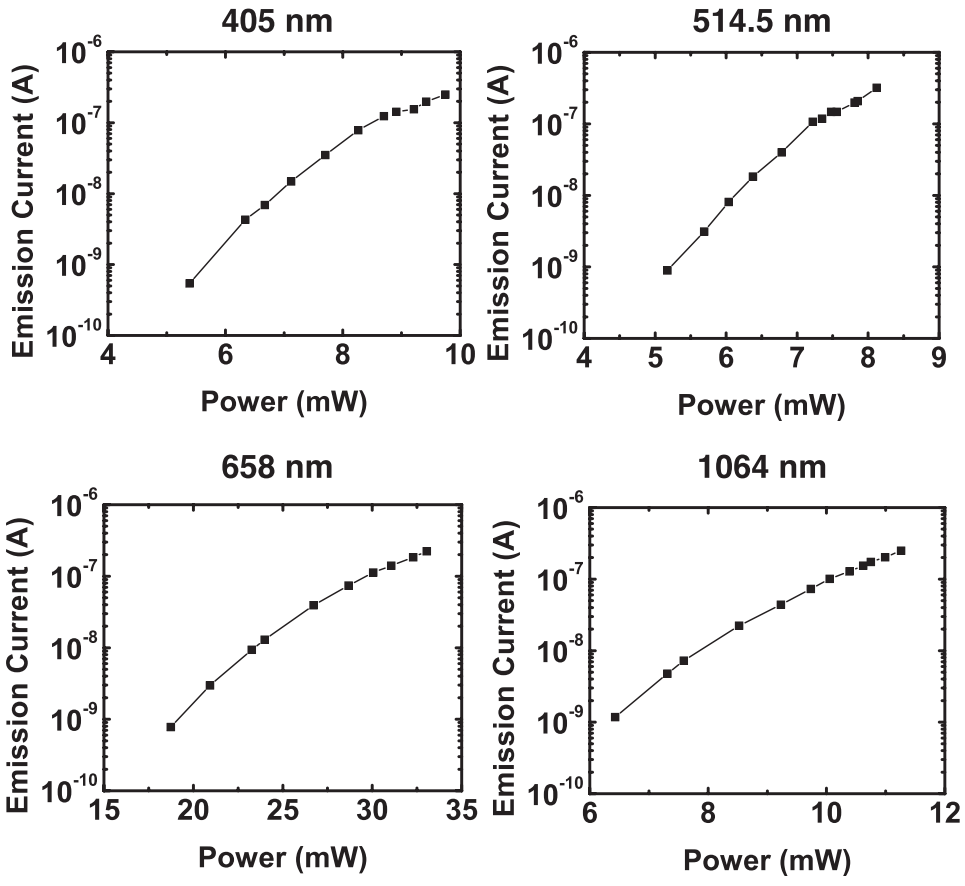

FIG. 2. Log-linear plots of electron emission current as a function of laser power for laser wavelengths of 405 nm, 514.5 nm, 658 nm, and 1064 nm. In all cases, the laser beam was focused to a spot in the range of 100-200 μm in diameter. All visible laser beams had an elliptical shape, with the 514.5-nm and 658-nm spot areas being ~0.8× and ~3.4× the area of the 405-nm spot, respectively. Our camera did not allow us to image the profile of the infrared beam.

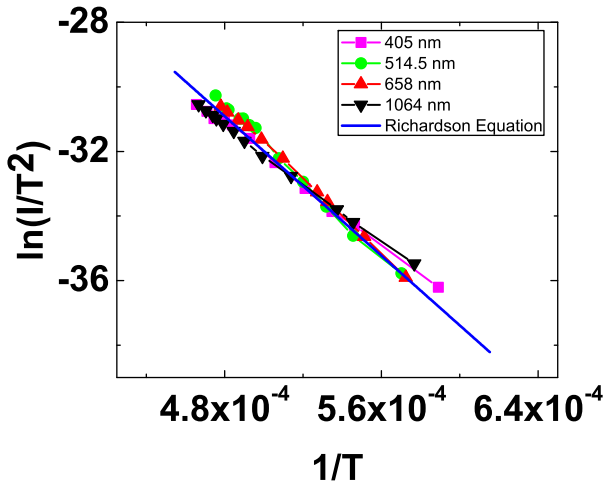

FIG. 3. Richardson plot for the electron emission current from the CNT forest induced by the 405-nm, 514.5-nm, 658-nm, and 1064-nm lasers, as well as the current calculated using the Richardson-Dushman equation (a work-function of 4.6 eV was used to obtain this reasonable fit to the experimental data). The temperatures were estimated using a power equilibrium condition as discussed in Ref. 8.

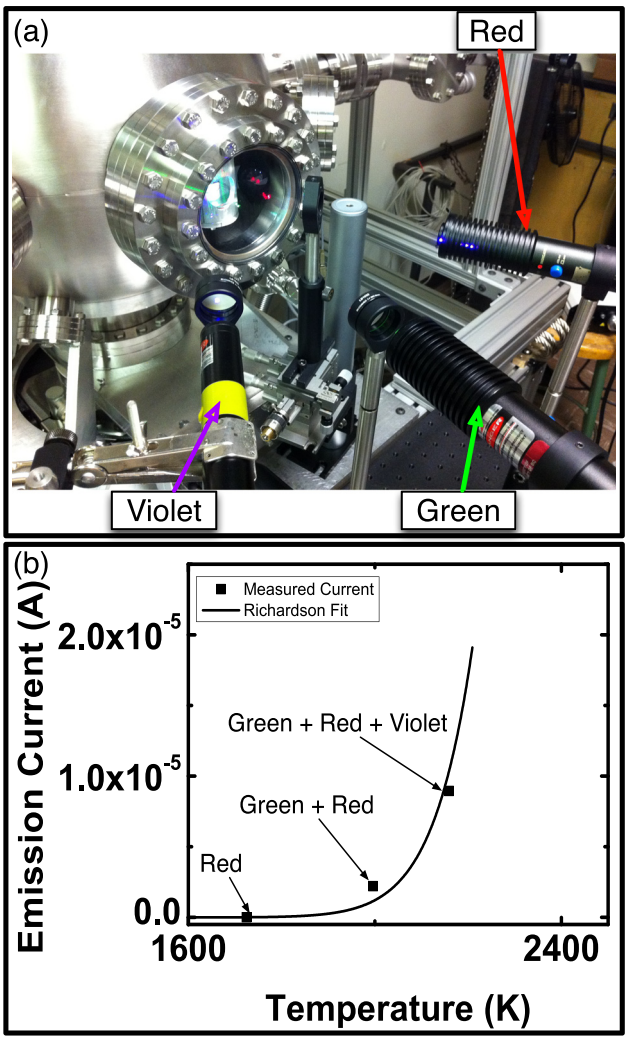

FIG. 4. (a) Multiple laser beams with different wavelengths being focused onto a single spot. (b) Emission current as a function of temperature for different combinations of laser wavelengths. The squares represent measured data and the line is a Richardson fit. The temperatures were estimated using a power equilibrium condition as discussed in Ref. 8.

TABLE I. Emission currents as a result of individual lasers and their combinations.

Wavelength	Power	Emission current
Violet	40 mW	14 nA
Green	45 mW	33 nA
Red	150 mW	1.5 nA
Green + red	…	2.2 μA
Green + red + violet	…	9 μA

Richardson equation. This indicates that adding beams with different wavelengths simply acts as adding the power of those lasers together. This behaviour is reasonable since CNTs are known to have high optical absorption over a wide range of wavelengths.

Figure 5 shows the thermionic emission current as a function of laser power for both polarizations of the 514.5-nm beam. At any given laser power, the current due to the s-polarized beam is significantly higher than that due to the p-polarized beam and, at high laser powers, this difference is over two orders of magnitude. Unlike with s-polarization where the current quickly ramps up, in the case of p-polarization, the initial increase in current is more gradual. The minimum current observed in our experiments was 0.5 nA, which was recorded at 5 mW of the 514.5-nm laser with p-polarization. Below this laser power, the electron emission current was negligible. The maximum laser power and emission current were limited to significantly below the point of destruction of the CNTs.

The effect of the polarization angle (the angle shown in Figure 1 inset) of the incident beam on electron emission was also measured for the two different wavelengths of 514.5 nm and 1064 nm (Figure 6). The angle was changed from 0°, where the electric field of the laser was perpendicular to the CNTs' axis (p-polarization) to 90°, where it was parallel to the CNTs' axis (s-polarization). The electron emission current for both wavelengths increased gradually as a function of the angle up to the point where the electric field

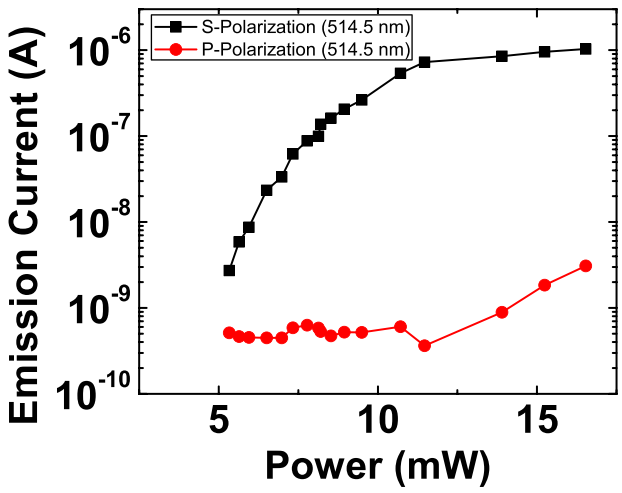

FIG. 5. Thermionic emission current from a CNT forest as a function of laser power for the two cases where the electric field of the laser was parallel and perpendicular to the CNTs' axis (black and red curves, respectively). The laser wavelength was 514.5 nm and the beam was perpendicular to the surface of the sidewall of the forest, focused to a spot of approximately 0.1 mm in diameter.

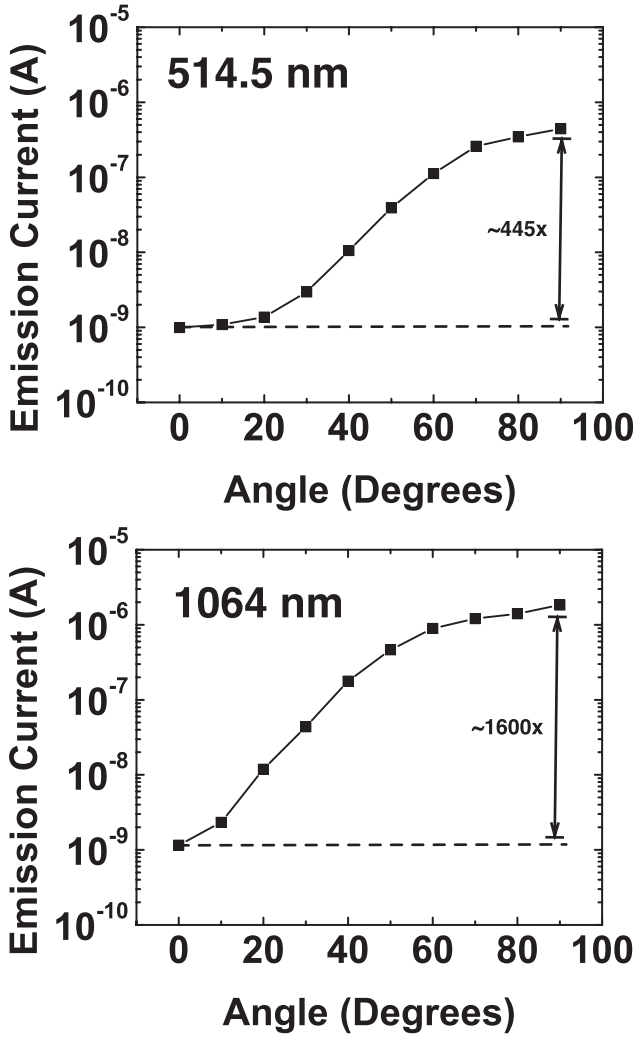

FIG. 6. Thermionic electron emission current as a function of the polarization angle for the 514.5-nm and 1064-nm lasers. 0° indicates the case where the electric field of the laser beam is perpendicular to the axis of the CNTs. The laser power was 7.7 mW for the 514.5-nm-beam and 13.8 mW for the 1064-nm-beam, so that both curves had a similar starting point in terms of emission current, in order to ease the comparison.

of the incident beam was entirely parallel to the CNTs' axis. At the longer laser wavelength of 1064 nm, the emission current appears to be more sensitive to polarization. The ratio of the emission currents resulting from s- and p-polarizations for the 1064-nm beam is over 3 times larger than the same ratio for the 514.5-nm beam. One potential reason behind the apparent higher sensitivity of the longer-wavelength case to polarization may be the difference in the polarization ratios of the two lasers; using an external polarizer, we ensured a polarization ratio of $>1000:1$ for both lasers to minimize this effect, although we could not eliminate it entirely. Assuming that this experimental non-ideality is not the main cause of the difference in behaviour observed between the two wavelengths, we offer the following explanation for this difference: We have previously simulated the optical absorption behavior in CNT forests[10] and observed that s-polarized light is mostly absorbed within a few tens of nanometers of the surface, while p-polarized light penetrates hundreds of nanometers or even micrometers (Figures 7(a) and 7(b)). For longer wavelengths, the penetration is deeper for both polarizations. Nonetheless, in the case of s-polarization, most of

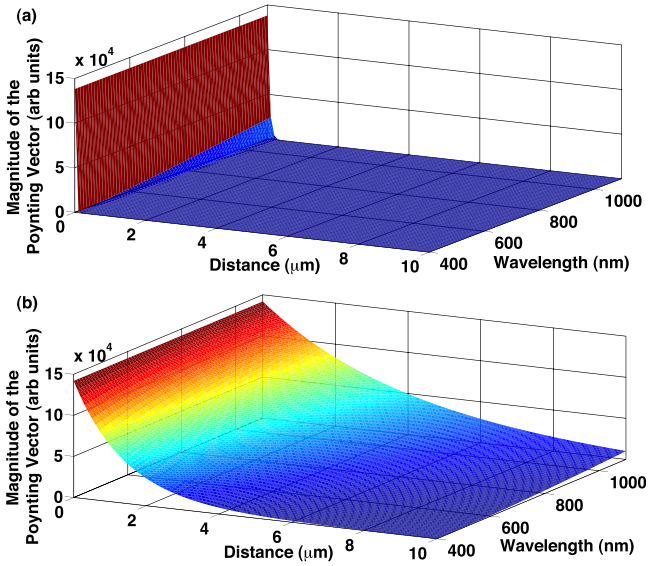

FIG. 7. Simulated magnitude of the Poynting vector as a function of wavelength and depth of light-penetration into the CNT forest for incident s- (a) and p- (b) polarized lights.

the light is absorbed near the surface (within a few nanotube layers) for both the 514.5-nm and 1064-nm lasers (see Figure 7(a)), where the thermionically-emitted electrons can easily escape. However, for p-polarization, the effect of deeper penetration of the longer-wavelength light becomes significant. For instance, as can be seen in Figure 7(b), over half of the 514.5-nm light is absorbed within the first 2 μm, but the 1064-nm light penetrates more than 4 μm before decaying to a similar value. Correspondingly, the resulting heat is also distributed more deeply into the forest for the longer wavelength, and a more significant portion of the electrons emitted due to the thermionic effect originate from deeper layers. These electrons cannot escape the sample as easily, leading to an overall lower emission current for p-polarized light at longer wavelengths.

We demonstrated that carbon nanotube forests can act as a thermionic electron source with a variety of wavelengths ranging from visible to infrared. The electron emission from the carbon nanotube forest is mainly thermionic in nature, achieved by efficient heating of the nanotubes through the "Heat Trap" effect. The electron emission current strongly depends on the polarization of the laser: the emission current is highest when the electric field of the laser is parallel to the axis of the nanotubes, in which case the emission current is relatively insensitive to laser wavelength. We also observed that at greater laser wavelengths, perpendicular polarization becomes less effective.

We acknowledge financial support from the Natural Sciences and Engineering Research Council, the Canada Foundation for Innovation, the British Columbia Knowledge Development Fund, the BCFRST Foundation, and the British Columbia Innovation Council. Parham Yaghoobi thanks the Department of Electrical and Computer Engineering and the University of British Columbia (UBC) for additional support.

[1]B. Barwick, H. S. Park, O.-H. Kwon, J. S. Baskin, and A. H. Zewail, Science **322**, 1227 (2008).

[2]S. H. Kong, J. Kinross-Wright, D. C. Nguyen, and R. L. Sheffield, Nucl. Instrum. Methods Phys. Res. A **358**, 272 (1995).
[3]J. W. Schwede, I. Bargatin, D. C. Riley, B. E. Hardin, S. J. Rosenthal, Y. Sun, F. Schmitt, P. Pianetta, R. T. Howe, Z.-X. Shen, and N. A. Melosh, Nature Mater. **9**, 762 (2010).
[4]J. S. Escher, G. A. Antypas, and J. Edgecumbe, Appl. Phys. Lett. **29**, 153 (1976).
[5]Y. Murakami, E. Einarsson, T. Edamura, and S. Maruyama, Phys. Rev. Lett. **94**, 087402 (2005).
[6]G. Fanchini, S. Miller, B. B. Parekh, and M. Chhowalla, Nano Lett. **8**, 2176 (2008).
[7]P. Yaghoobi, M. V. Moghaddam, M. Michan, and A. Nojeh, J. Vac. Sci. Technol. B **29**, 02B104 (2011).
[8]P. Yaghoobi, M. V. Moghaddam, and A. Nojeh, Solid State Commun. **151**, 1105 (2011).
[9]O. W. Richardson, Proc. Cambridge Philos. Soc. **11**, 286 (1901).
[10]P. Yaghoobi, M. Michan, and A. Nojeh, Appl. Phys. Lett. **97**, 153119 (2010).